NATIONAL ADVISORY COMMITTEE FOR AERONAUTICS

TECHNICAL NOTE 1947

INVESTIGATION OF FLOW COEFFICIENT OF CIRCULAR, SQUARE, AND ELLIPTICAL ORIFICES AT HIGH PRESSURE RATIOS

By Edmund E. Callaghan and Dean T. Bowden

Lewis Flight Propulsion Laboratory
Cleveland, Ohio

Washington
September 1949

NATIONAL ADVISORY COMMITTEE FOR AERONAUTICS

TECHNICAL NOTE 1947

INVESTIGATION OF FLOW COEFFICIENT OF CIRCULAR, SQUARE, AND ELLIPTICAL ORIFICES AT HIGH PRESSURE RATIOS

By Edmund E. Callaghan and Dean T. Bowden

SUMMARY

An experimental investigation has been conducted to determine the orifice coefficient of a jet directed perpendicularly to an air stream as a function of pressure ratio and jet Reynolds number for circular, square, and elliptical orifices. The effect of air-stream velocity on the jet flow was also determined for three tunnel-air velocities. Equations for the flow coefficients in terms of jet Reynolds number and pressure ratio were obtained for the various shapes. Excellent correlation was obtained between the results for a jet discharging into still air and the results for a jet discharging into a moving air stream, provided that the correct outlet pressure was used.

INTRODUCTION

The introduction of a gas or a vapor into an air stream for purposes of heating or cooling the air stream may be easily accomplished by the use of a high-velocity jet directed perpendicularly to the air stream, as reported in reference 1. In order to evaluate the heating or cooling effect of such a jet, knowledge of the mass air flow of the jet or, more fundamentally, the discharge coefficient of the orifice from which the jet is issuing is essential. In addition to the effects of jet Reynolds number and orifice shape on the discharge coefficient, the jet pressure ratio and the interaction of the air stream and the jet must be considered.

An investigation to determine the orifice-discharge coefficient of a high-velocity air jet directed perpendicularly to an air stream was undertaken in a 2- by 20-inch duct tunnel at the NACA Lewis laboratory. The discharge coefficients of circular, square, and elliptical orifices were determined at tunnel-air velocities of 160, 275, and 380 feet per second for several jet (orifice) areas, a range of pressure ratios from 1.15 to 3.2, and a jet total temperature of approximately 400° F.

APPARATUS AND PROCEDURE

The experimental investigation consisted of two parts: (1) determination of the flow coefficients of the orifices in still air, and (2) determination of the effect of tunnel-air velocity on the jet flow.

Flow coefficients in still air. - The nine 1/16-inch-thick thin-plate orifices investigated consisted of three circles, two ellipses with an axis ratio of 4:1, two ellipses with an axis ratio of 2:1, and two squares. The circular orifices had diameters of 0.375, 0.500, and 0.625 inch; the ellipses and squares had areas equivalent to the 0.375- and 0.625-inch-diameter circles. Each orifice was investigated over a range of pressure ratios from 1.15 to 3.2 and for jet total temperatures of approximately 70° and 400° F. Air for the jets was obtained by passing high-pressure air through an electric heater and into a plenum chamber, the upper wall of which contained the orifice, as shown in figure 1. The mass flow was measured by a calibrated orifice in the ducting upstream of the heater. The calibration curve for the measuring orifice indicated an over-all accuracy of 2 percent.

The plenum chamber was constructed with an inside diameter of 6 inches to minimize the effect of approach velocity and to insure that the static temperature and pressure measured in the plenum chamber would be equal to the total temperature and pressure of the jet at the vena contracta.

Static pressures were measured at the orifice and at a point upstream of the orifice by pressure taps in the tunnel walls.

Effect of tunnel-air velocity on jet. - The elliptical orifices were mounted with the major axis parallel to the air stream and the square orifices with two edges parallel to the air stream. Each of the nine orifices was investigated over a range of pressure ratios from 1.15 to 3.2 for a jet total temperature of 400° F and at tunnel-air velocities of 160, 275, and 380 feet per second. The static pressure was measured by the wall taps used in the static investigation and later by a static tap located in the tunnel floor at the point of maximum thickness of the jet and about 0.030 inch from the orifice.

SYMBOLS

The following symbols are used in this report:

a_j	speed of sound at jet vena contracta, feet per second
b	minor axis of elliptical orifice, feet
C	flow coefficient, ratio of measured to theoretical flow
D_j	diameter of circular orifice, feet
d	length of side of square orifice, feet
g	acceleration due to gravity, 32.2 feet per second per second
P_j	total pressure of jet, pounds per square foot absolute
p_j	outlet static pressure immediately adjacent to orifice, pounds per square foot absolute
p_p	static pressure of air in plenum chamber, pounds per square foot absolute
R	gas constant, 53.3 foot-pounds per pound per $^{\circ}F$
Re	jet Reynolds number
T_j	total temperature of jet, $^{\circ}F$
t_p	static temperature of air in plenum chamber, $^{\circ}R$
V_j	velocity of jet at vena contracta, feet per second
V_p	velocity of air in plenum chamber, feet per second
θ, β	flow parameters
γ	ratio of specific heats of air, 1.400
μ_j	viscosity of jet at vena contracta, slugs per foot per second
ρ_j	mass density of jet at vena contracta, slugs per cubic foot
ρ_p	mass density of air in plenum chamber, slugs per cubic foot

METHODS OF CALCULATION

The jet velocity V_j and the jet density ρ_j at the vena contracta, or minimum section, were determined with the compressible-flow relations for the subsonic or unchoked conditions from the following equations:

$$\frac{\gamma}{\gamma-1}\frac{p_p}{\rho_p} + \frac{V_p^2}{2} = \frac{\gamma}{\gamma-1}\frac{p_j}{\rho_j} + \frac{V_j^2}{2}$$

$$\frac{\rho_j}{\rho_p} = \left(\frac{p_j}{p_p}\right)^{\frac{1}{\gamma}}$$

Because V_p is very near zero, $p_p = p_j$ and $t_p = T_j + 460$ and therefore

$$V_j = \sqrt{\frac{2\gamma}{\gamma-1}\left(\frac{p_p}{\rho_p} - \frac{p_j}{\rho_j}\right)} = 2.646\sqrt{\frac{p_p}{\rho_p} - \frac{p_j}{\rho_j}}$$

$$\rho_j = \rho_p\left(\frac{p_j}{p_p}\right)^{\frac{1}{\gamma}}$$

When the static-pressure ratio across the jet exceeded that necessary for choking, the jet velocity at the vena contracta equaled the local speed of sound in the air. The jet velocity for this case was determined from the following equation:

$$V_j = a_j = \sqrt{\frac{2\gamma}{\gamma+1}\,gR(T_j + 460)} = 44.8\sqrt{T_j + 460} = 44.8\sqrt{t_p}$$

The jet density for the choked condition was determined from the total temperature and pressure by use of the following equation:

$$\rho_j = \left(\frac{\gamma+1}{2}\right)^{\frac{1}{1-\gamma}} 0.000583\,\frac{P_j}{T_j + 460} = 0.000369\,\frac{P_j}{T_j + 460} = 0.000369\,\frac{p_p}{t_p}$$

The theoretical mass flow of the jet was calculated as the product of the jet density ρ_j, the jet velocity V_j, and the orifice area. The flow coefficient C was calculated as the ratio of measured flow to theoretical flow.

RESULTS AND DISCUSSION

The problem of orifice-discharge coefficients at high pressure ratios was first investigated by de Saint-Venant (reference 2) and later in references 3 to 5. A theoretical analysis was presented in 1902 by Chaplygin (reference 6) that showed good agreement with the results of references 3 to 5. All the experimental investigations, however, were conducted with circular orifices in still air and no attempt was made to obtain a jet Reynolds number correlation or shape effect. In addition, when a jet is discharged into a moving air stream, an interaction between the stream and the jet may be expected.

Jets discharging into still air. - The first part of the investigation was conducted to determine the orifice coefficients of a jet discharging into still air. The variation of flow coefficient as a function of pressure ratio P_j/p_j is shown in figure 2 for the 0.375- and 0.625-inch-diameter circular orifices at a constant jet total temperature of 70° F. The slight offset of the similar curves obtained indicates a jet Reynolds number effect. This effect may also be seen in figure 3, where flow coefficients for the 0.625-inch-diameter orifice are plotted as a function of pressure ratio for jet total temperatures of 70° and 400° F.

In both figures 2 and 3, the effect of increasing the Reynolds number, either by using a larger orifice diameter or a lower jet temperature, yields a lower flow coefficient.

The curves of figures 2 and 3 show that a linear variation of flow coefficient was obtained with pressure ratio at subsonic flows. A transition region occurred at pressure ratios slightly higher than choking flow (1.87) and a definite decrease in slope of the curve was evident. A linear variation of flow coefficient with pressure ratio was again obtained at high values of pressure ratio.

A cross plot of all the circular-orifice data is shown in figure 4 where the flow coefficient is plotted as a function of jet Reynolds number $(\rho_j V_j D_j)/\mu_j$ for constant values of pressure ratio.

The curves obtained are similar to those normally given for orifice-discharge coefficients at pressure ratios near 1. The flow coefficient decreased with increasing jet Reynolds number.

A cross plot of the data in figure 4 showed that at a constant Reynolds number two straight lines almost exactly represented the variation of flow coefficient with pressure ratio (fig. 5).

These flow-coefficient relations at constant Reynolds number were utilized as a parameter θ. From a replot of the data in figure 4 as the variation of flow parameter C/θ with Reynolds number, a single curve was obtained (fig. 6). An equation for this curve has been obtained; it should be noted, however, that θ represents two functions that are valid only in their defined limits.

$$\frac{C}{\theta} = 0.948 + \frac{4.83}{Re \times 10^{-4} + 53.8}$$

where for P_j/p_j from 1.15 to 2.09

$$\theta = 0.151 \frac{P_j}{p_j} + 0.44$$

and for P_j/p_j from 2.09 to 3.2

$$\theta = 0.060 \frac{P_j}{p_j} + 0.636$$

and

$$Re = \frac{\rho_j V_j D_j}{\mu_j}$$

Two curves of flow coefficient as a function of pressure ratio have been constructed from this equation for Reynolds numbers of 60,000 and 350,000 and plotted with the theoretical results presented by Chaplygin (fig. 7). The analysis of reference 6 is applicable only for two-dimensional flow in the subsonic region. The agreement between the theoretical calculations for two-dimensional flow and the experimental results for three-dimensional subsonic flow is evident in figure 7.

Analysis of the elliptical data showed that it was possible to correlate the flow coefficients of the ellipses with axis ratios of 4:1 and 2:1 as a function of jet Reynolds number for constant pressure ratios, provided that the jet Reynolds number was based on the minor axis. The variation of flow coefficient with Reynolds number at constant pressure ratios is shown in figure 8 for all four ellipses at jet total temperatures of 70° and 400° F.

A comparison of the curves in figure 8 at a constant value of Reynolds number showed that each curve had a slightly different slope. It was therefore necessary to obtain a parameter β in terms of the pressure ratio based on the Reynolds number at which identical slopes were obtained. A plot of the variation of flow coefficient with Re/β was made and curves similar to those for circular orifices were obtained. The parameter θ could then be obtained so that C/θ plotted as a function of Re/β yielded a single curve (fig. 9). The following equation for this experimental curve was obtained:

$$\frac{C}{\theta} = 0.964 + \frac{0.130}{\frac{Re \times 10^{-4}}{\beta} + 0.63}$$

for P_j/p_j from 1.15 to 2.09

$$\theta = 0.149 \frac{P_j}{p_j} + 0.469$$

$$\beta = 5.97 \frac{P_j}{p_j} - 4.17$$

and for P_j/p_j from 2.09 to 3.2

$$\theta = 0.054 \frac{P_j}{p_j} + 0.667$$

$$\beta = 2.00 \frac{P_j}{p_j} + 4.20$$

and

$$Re = \frac{\rho_j V_j b}{\mu_j}$$

The flow coefficients obtained with the square orifices were correlated with Reynolds number in the same manner as for the circular orifices (fig. 10). The Reynolds number was based on the length of a side d.

It was again possible to plot C/θ as a function of Reynolds number and obtain a single curve (fig. 11). The following equation for this experimental curve was obtained:

$$\frac{C}{\theta} = 0.916 + \frac{7.5}{Re \times 10^{-4} + 74.0}$$

where for P_j/p_j from 1.15 to 2.09

$$\theta = 0.150 \frac{P_j}{p_j} + 0.467$$

for P_j/p_j from 2.09 to 3.2

$$\theta = 0.061 \frac{P_j}{p_j} + 0.655$$

and

$$Re = \frac{\rho_j V_j d}{\mu_j}$$

A comparison of the various curves calculated from the orifice equations (fig. 12) shows that for a given orifice area, jet temperature, and outlet pressure, the flow coefficients in descending order were the ellipse with an axis ratio of 4:1, the ellipse with an axis ratio of 2:1, the square, and the circle. This relation of the various flow coefficients logically follows from considerations of the types of flow involved. With the circular orifice, the lines of flow converge from all azimuths and hence result in the lowest flow coefficients. The square-orifice flow lines converge in approximately four directions and thus should produce a higher flow

coefficient than a circular orifice. The ellipses, particularly those with large axis ratio, approach a slot in shape and therefore yield the highest flow coefficients because the flow lines from a slot converge in only two directions.

Effect of tunnel-air velocity on jet flow. - For the initial study of the interaction of the jet and the air stream, the static pressure into which the jet was discharging was assumed equal to the free-stream static pressure of the air stream. The variation of flow coefficient with pressure ratio is shown in figure 13 for a 0.625-inch-diameter circular orifice at a jet total temperature of 400° F and at tunnel-air velocities of 0, 160, 275, and 380 feet per second. Because the curves were separated by a function that was dependent on the free-stream velocity and because of the relation of static pressure to velocity (Bernoulli's equation), a further investigation of the static pressure into which the jet was discharging was undertaken.

Measurements were made of the static pressure immediately adjacent to the jet at the point of maximum thickness by a tap located in the tunnel 0.030 inch from the orifice. These data indicated a static pressure considerably lower than free stream and somewhat lower than that indicated by a static tap located on the tunnel wall at the same longitudinal position. Analysis of these data showed that the free-stream static pressure was related to the outlet static pressure in accordance with the Bernoulli and mass-flow equations, provided that the free area at the orifice was based on the tunnel width minus the jet width at the point of maximum thickness. When the data of figure 13 were replotted using the corrected values of flow coefficient and pressure ratio based on the corrected outlet pressure, data were obtained (fig. 14) that were in excellent agreement with the calculated curve for a jet discharging into still air. When this correction was applied to all the data for circular, square, and elliptical orifices, excellent agreement was obtained with the results for a jet discharging into still air. Calculation of the flow coefficient for a jet discharging into an air stream is thus possible when the equations for a jet discharging into still air are employed, provided that the correct outlet pressure is used.

SUMMARY OF RESULTS

The following results were obtained in the investigation of the flow coefficients of circular, square, and elliptical orifices discharging into both a still and a moving air stream.

1. Equations were obtained for the flow coefficients for the various shapes, in terms of pressure ratio and jet Reynolds number.

2. Agreement was obtained between the experimental results for three-dimensional flow with circular orifices and the theoretical results for two-dimensional flow.

3. The flow coefficient increased linearly with increasing pressure ratio for pressure ratios up to choking. A transition region was obtained at pressure ratios slightly higher than choking and the flow-coefficient variation again became linear with pressure ratio for the high values of pressure ratio.

4. The flow coefficient increased more rapidly at the low pressure ratios than at high pressure ratios.

5. The flow coefficient decreased with increasing jet Reynolds number at constant pressure ratios.

6. For a particular value of pressure ratio and jet total temperature, the ellipses yielded the highest flow coefficients.

7. No effect of stream velocity on flow coefficient was obtained, provided that the proper outlet static pressure was utilized.

Lewis Flight Propulsion Laboratory,
National Advisory Committee for Aeronautics,
Cleveland, Ohio, May 13, 1949.

REFERENCES

1. Callaghan, Edmund E., and Ruggeri, Robert S.: Investigation of the Penetration of an Air Jet Directed Perpendicularly to an Air Stream. NACA TN 1615, 1948.

2. de Saint-Venant, Barré, et Wantzel, Laurent: Mémoire et expériences sur l'écoulement de l'air. Jour. L'École Roy. Poly., T. XVI, Cahier 27, 1839, pp. 85-122.

3. Hirn: Réflexions sur une critique de M. Hugoniot, parue aux "Comptes rendus" du 28 Juin. Comptes Rendus, T. 103, Juil.-Déc. 1886, pp. 109-113; Résponse relative à la note de M. Hugoniot: "Sur la pression qui existe dans la section contractée d'une veine gazeuse", p. 371; Remarques au sujet des notes de M. Hugoniot, insérées aux "Comptes rendus" des 15 et 22 Nov., pp. 1232-1236.

4. Parenty, H.: Sur le débit des gaz parfaits et de la vapeur d'eau sous pression a travers les orifices. Ann. Chim. et Phys., T. VIII, Sér. VII, 1896, pp. 5-79.

5. Parenty, H.: Sur les vitesses, les températures et les poids spécifiques des gaz parfaits et de la vapeur d'eau s'écoulant a travers les orifices. Ann. Chim. et Phys., T. XII, Sér. 7, 1897, pp. 289-373.

6. Chaplygin, S.: Gas Jets. NACA TM 1063, 1944.

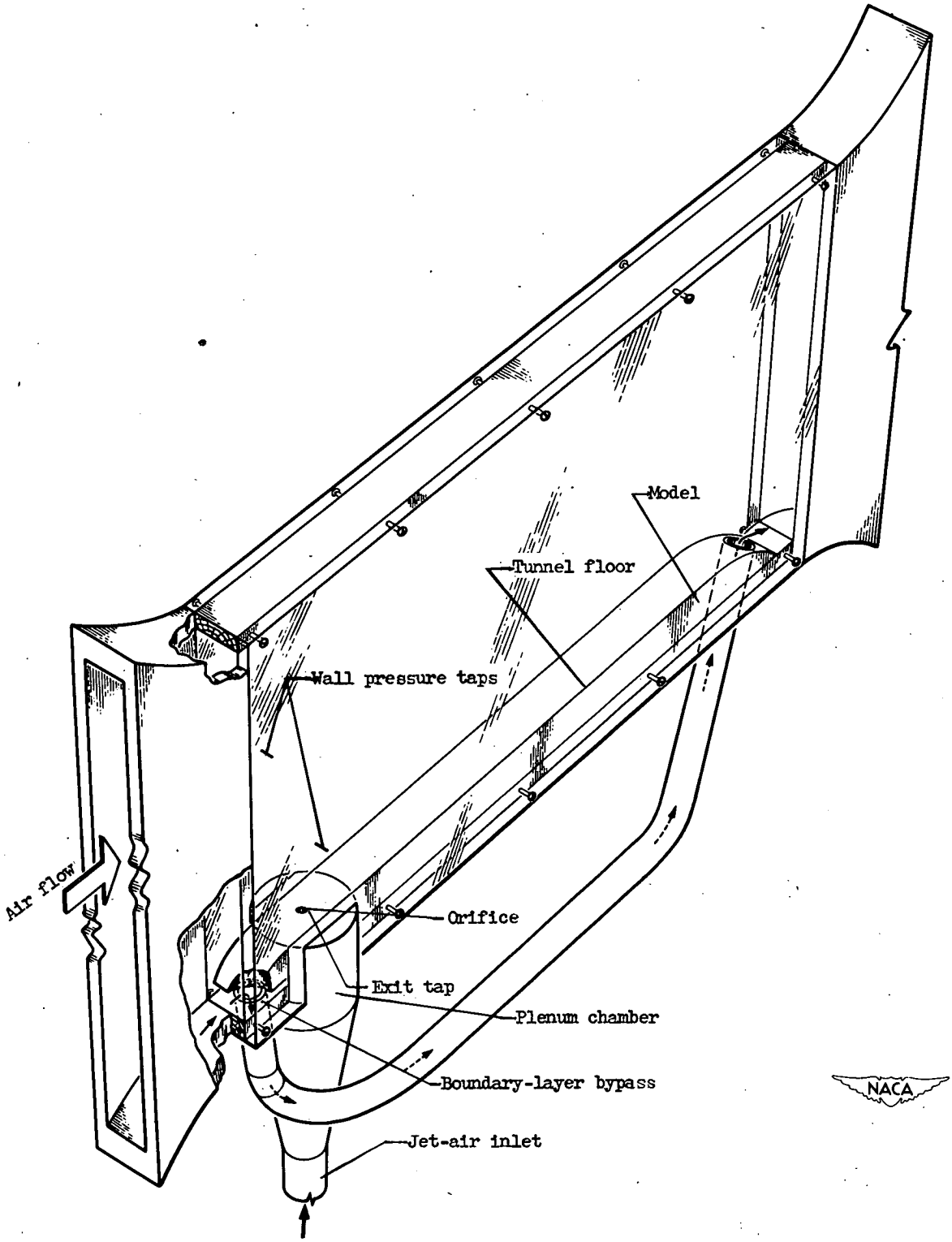

Figure 1. - Arrangement of orifice in plane parallel to air stream.

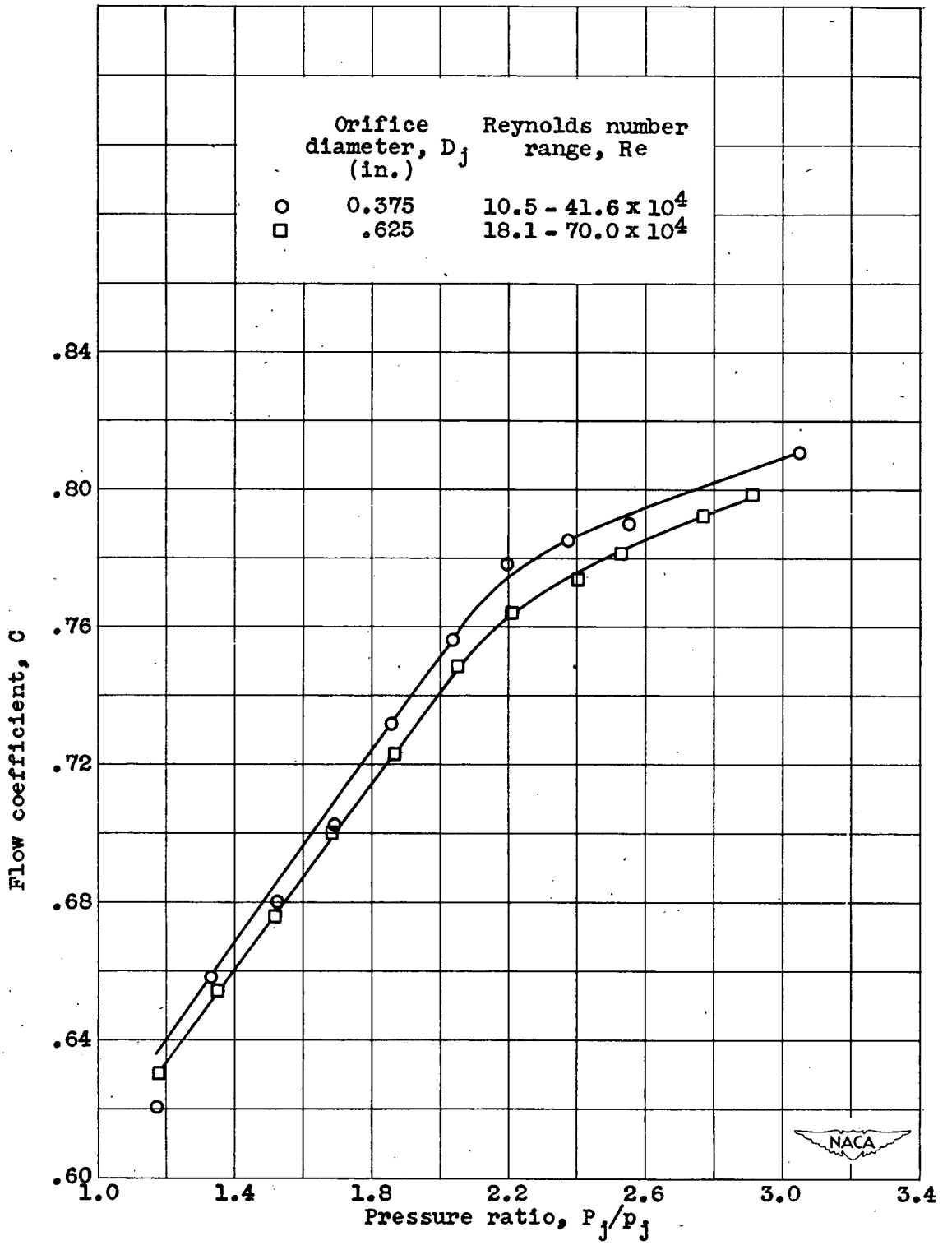

Figure 2. - Variation of flow coefficient with pressure ratio for two circular orifices at jet total temperature of 70° F.

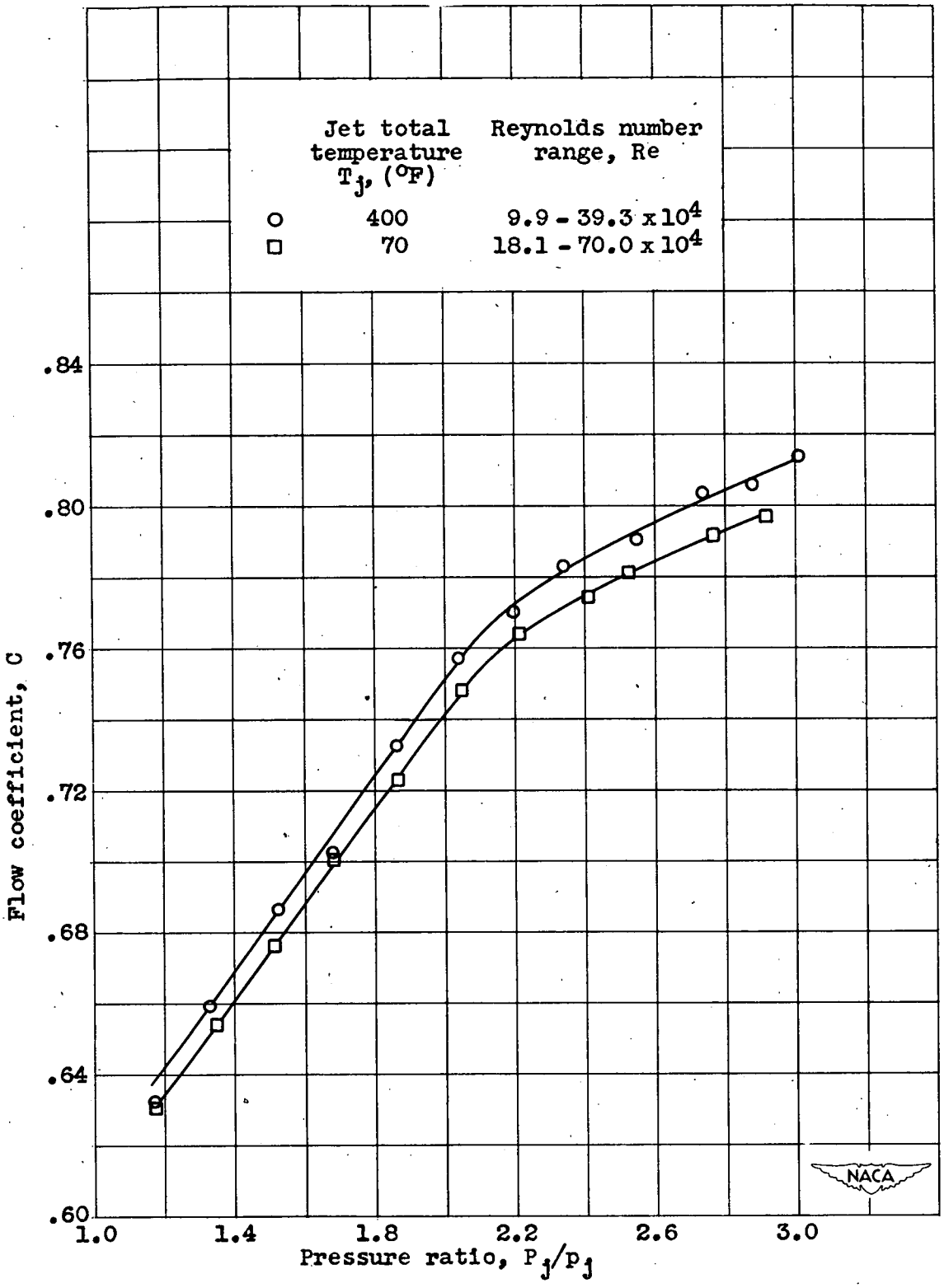

Figure 3. - Variation of flow coefficient with pressure ratio for 0.625-inch circular orifice.

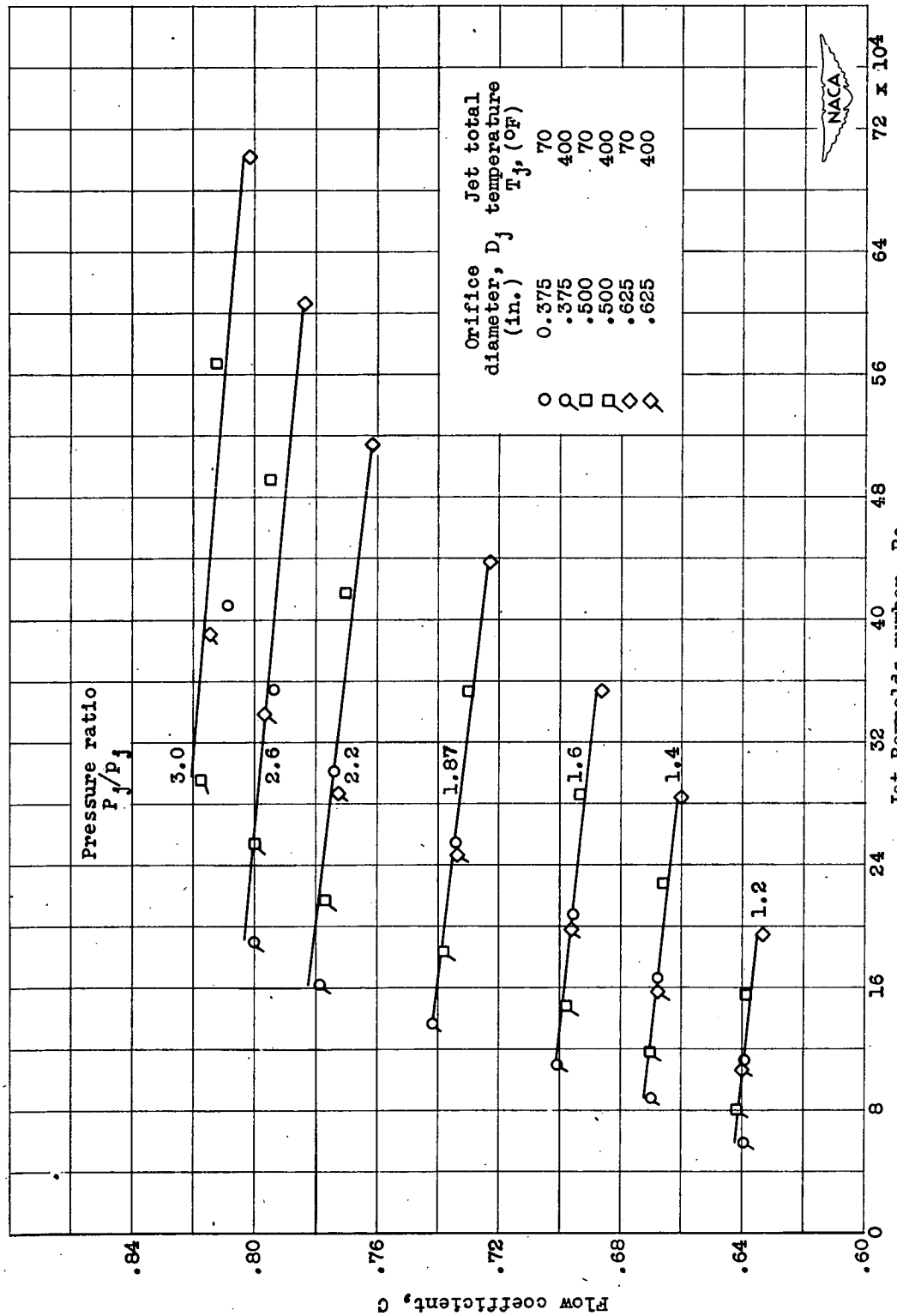

Figure 4. - Variation of flow coefficient at constant pressure ratios with Reynolds number for circular orifices.

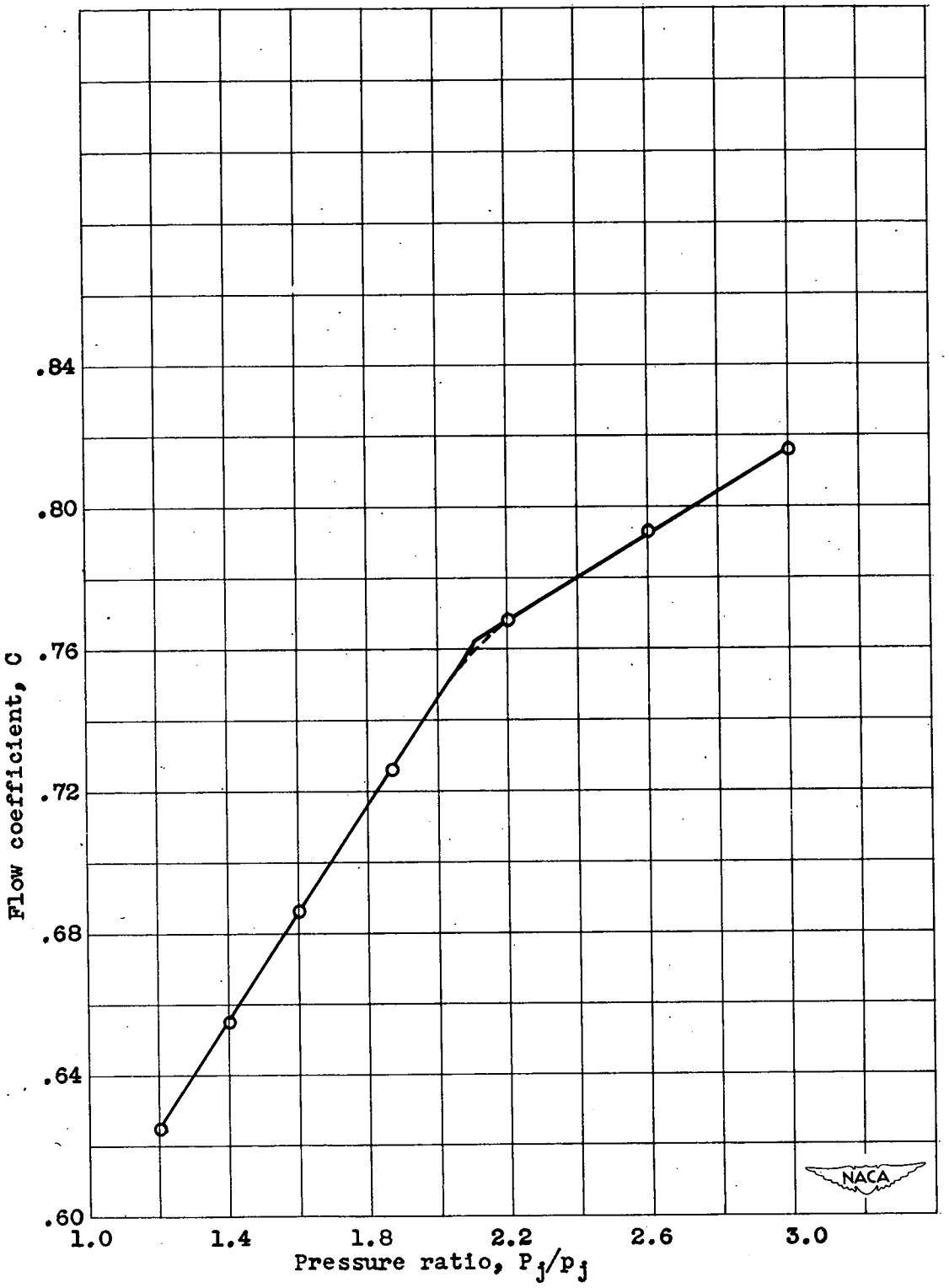

Figure 5. - Variation of flow coefficient with pressure ratio at constant Reynolds number of 400,000 for circular orifices.

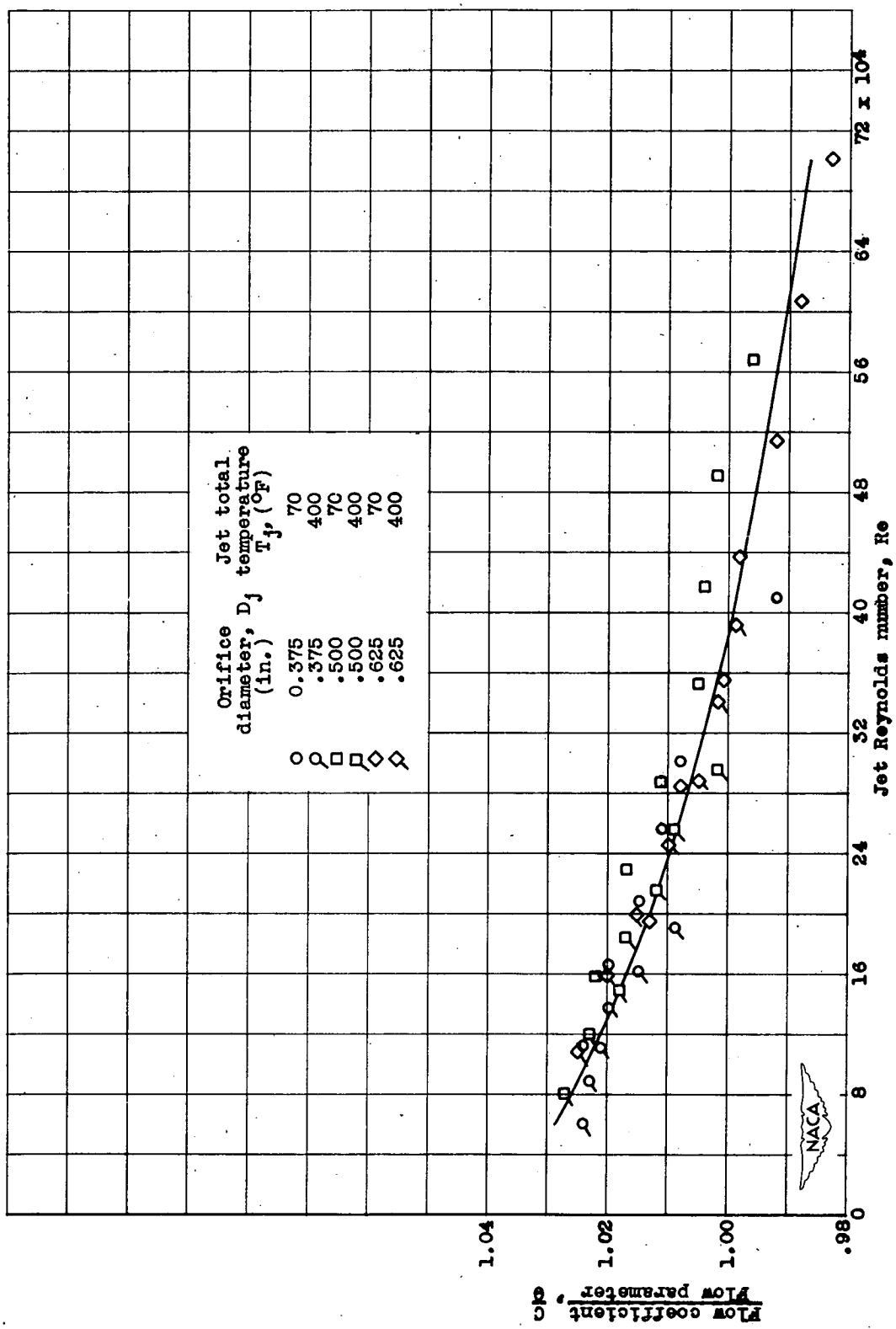

Figure 6. - Variation of ratio of flow coefficient to flow parameter θ with Reynolds number for circular orifices.

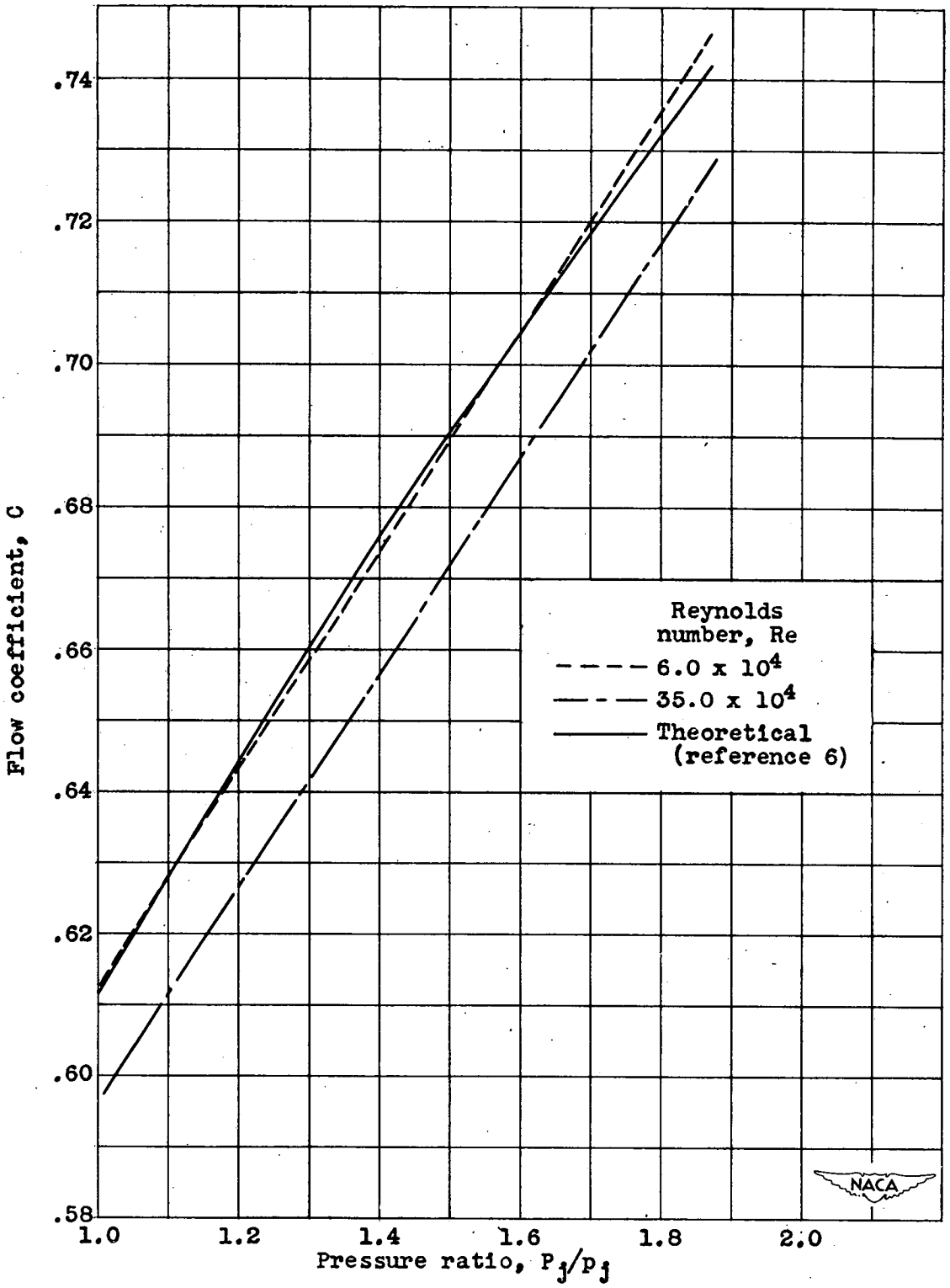

Figure 7. - Comparison of flow-coefficient variation with pressure ratio for two Reynolds numbers with results of reference 6.

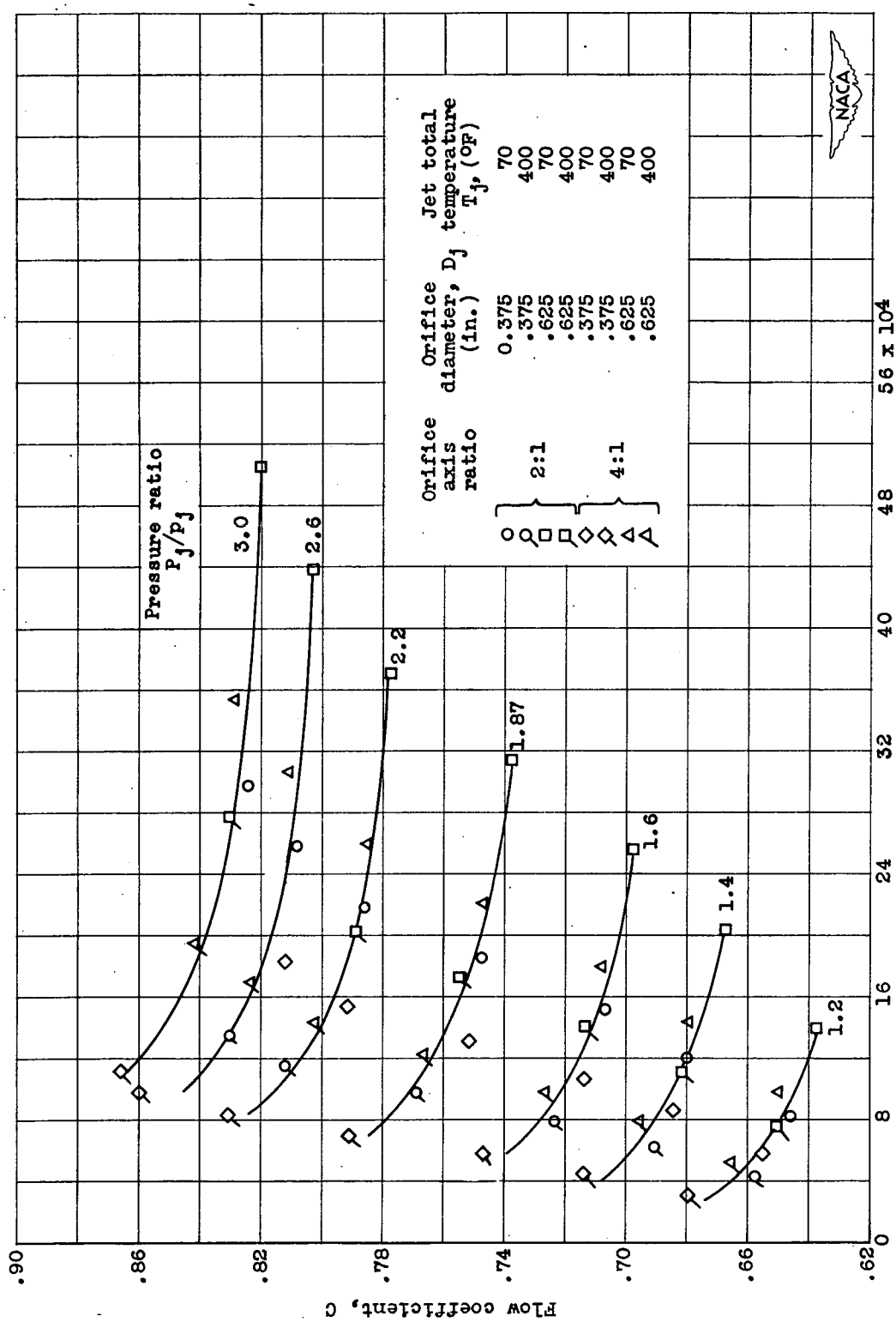

Figure 8. - Variation of flow coefficient at constant pressure ratios with Reynolds number for elliptical orifices.

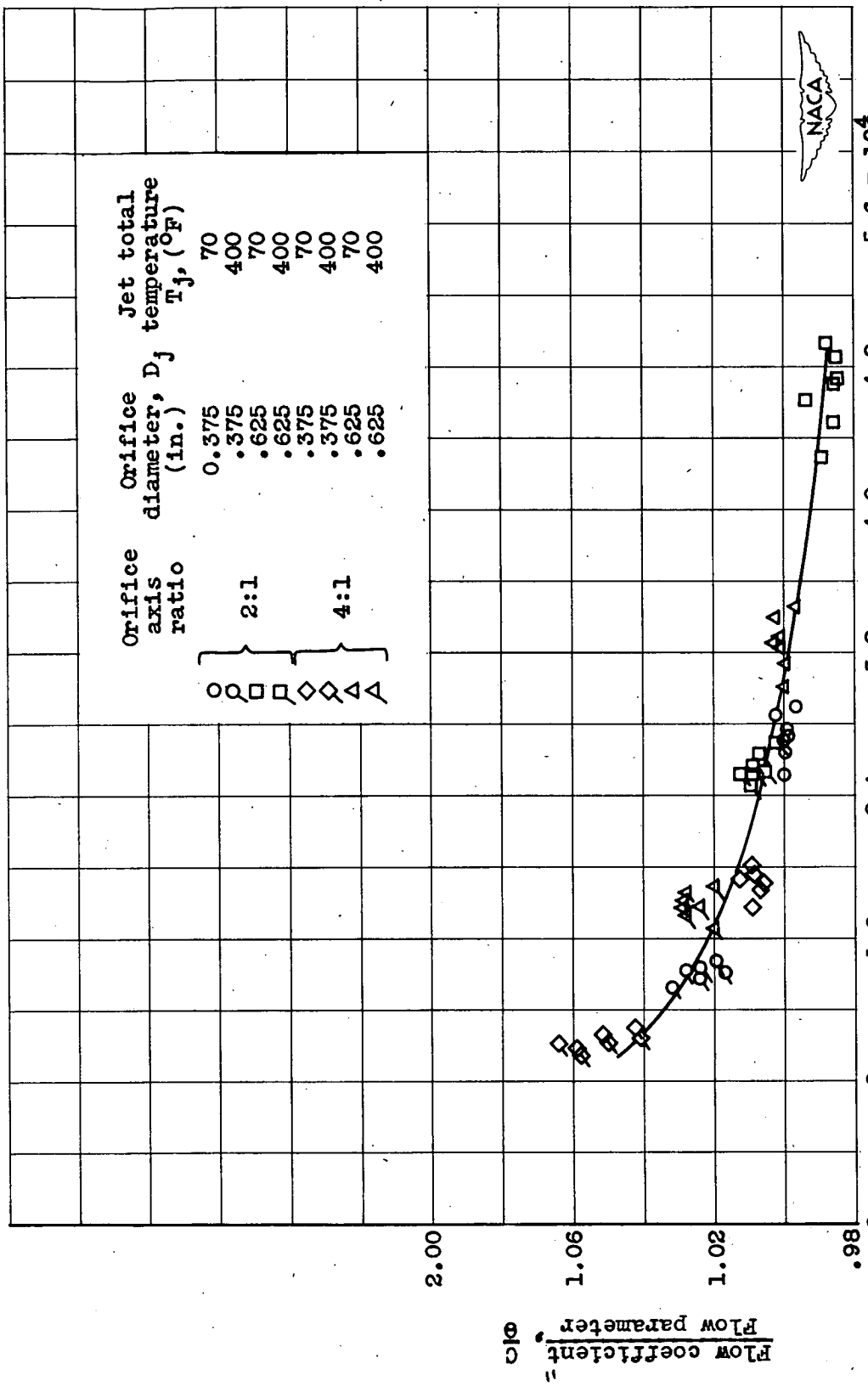

Figure 9. - Variation of ratio of flow coefficient to flow parameter θ with ratio of Reynolds number to flow parameter β.

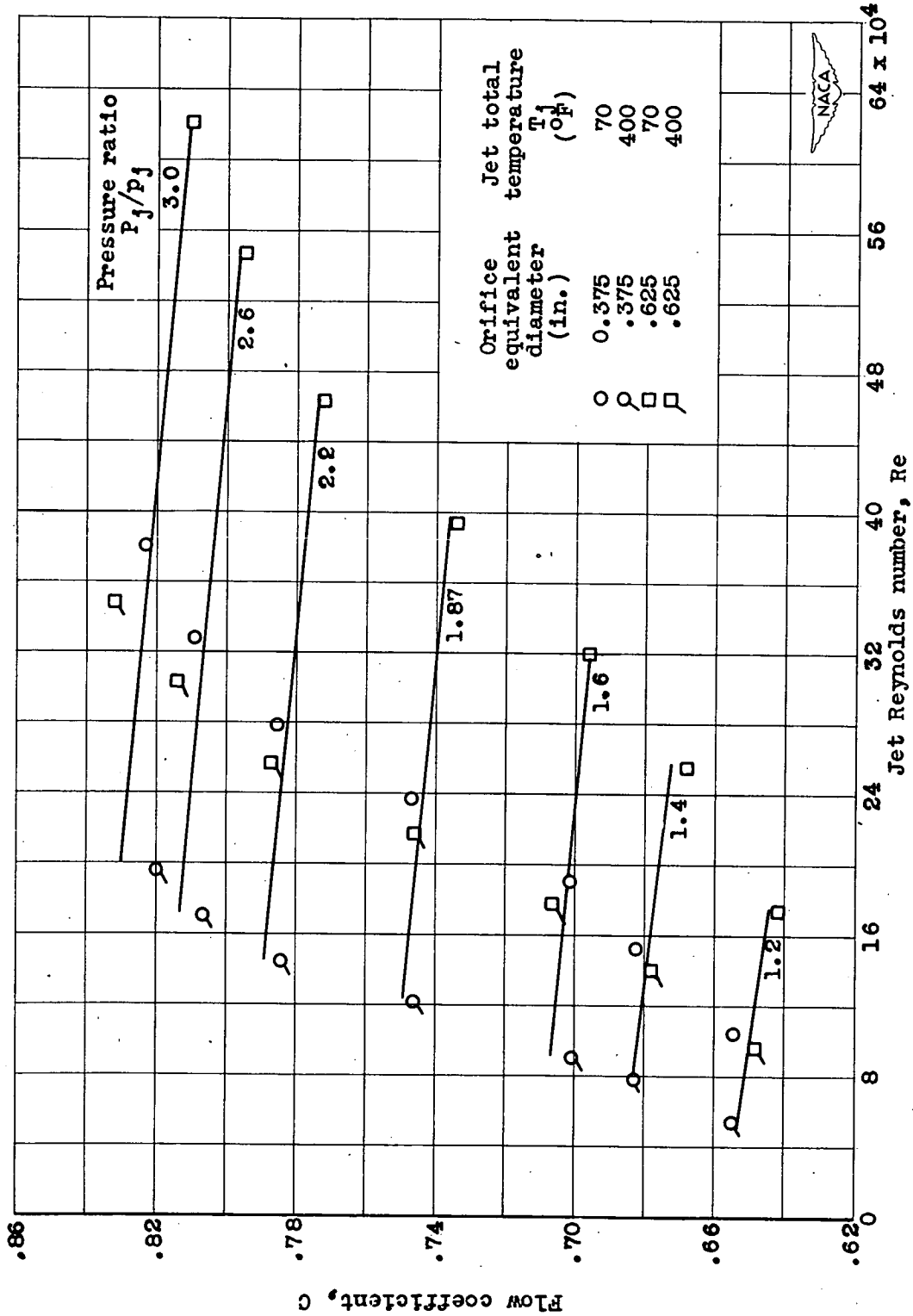

Figure 10. - Variation of flow coefficient at constant pressure ratios with Reynolds number for square orifices.

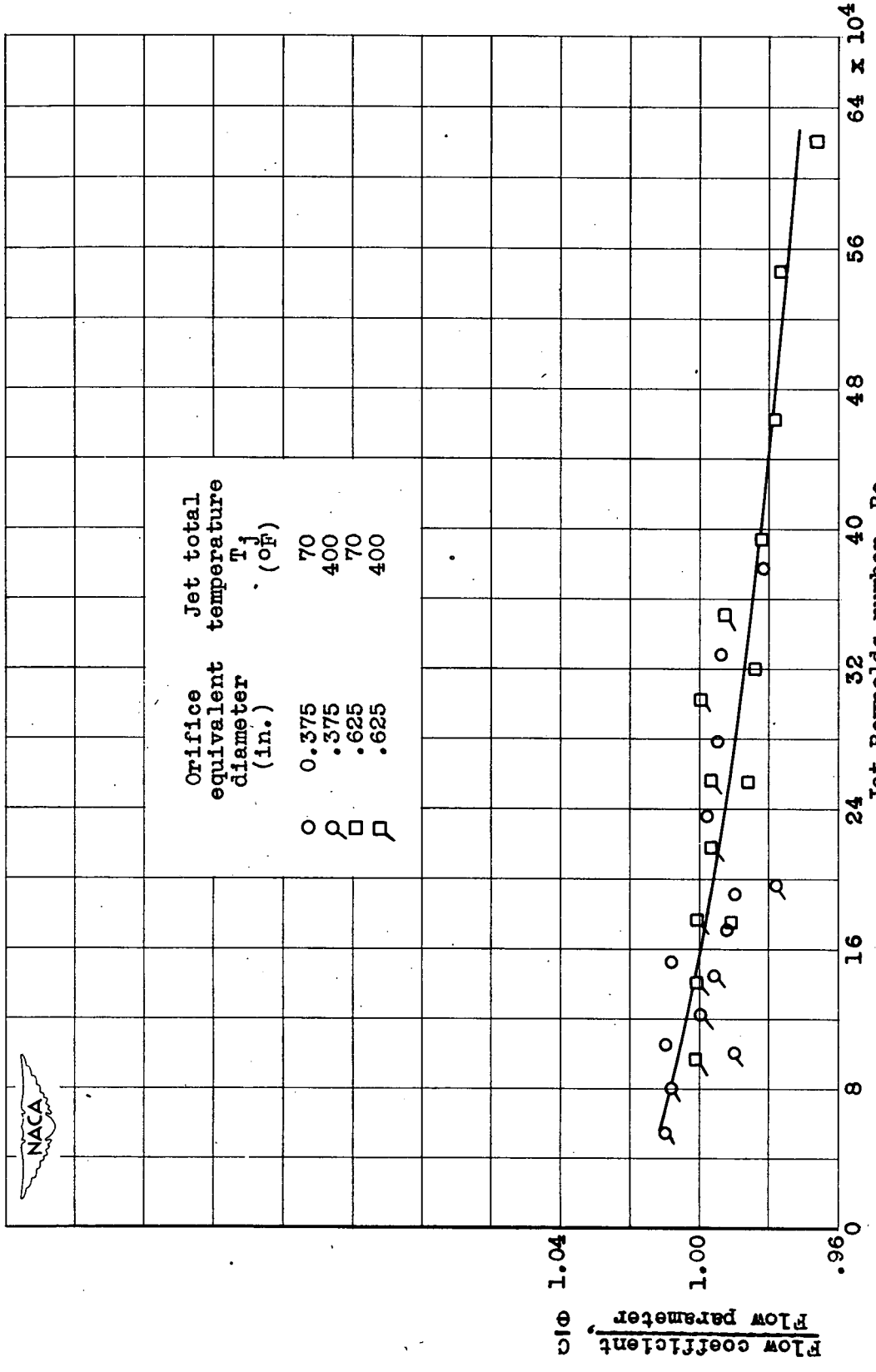

Figure 11. - Variation of ratio of flow coefficient to flow parameter θ with Reynolds number for square orifices.

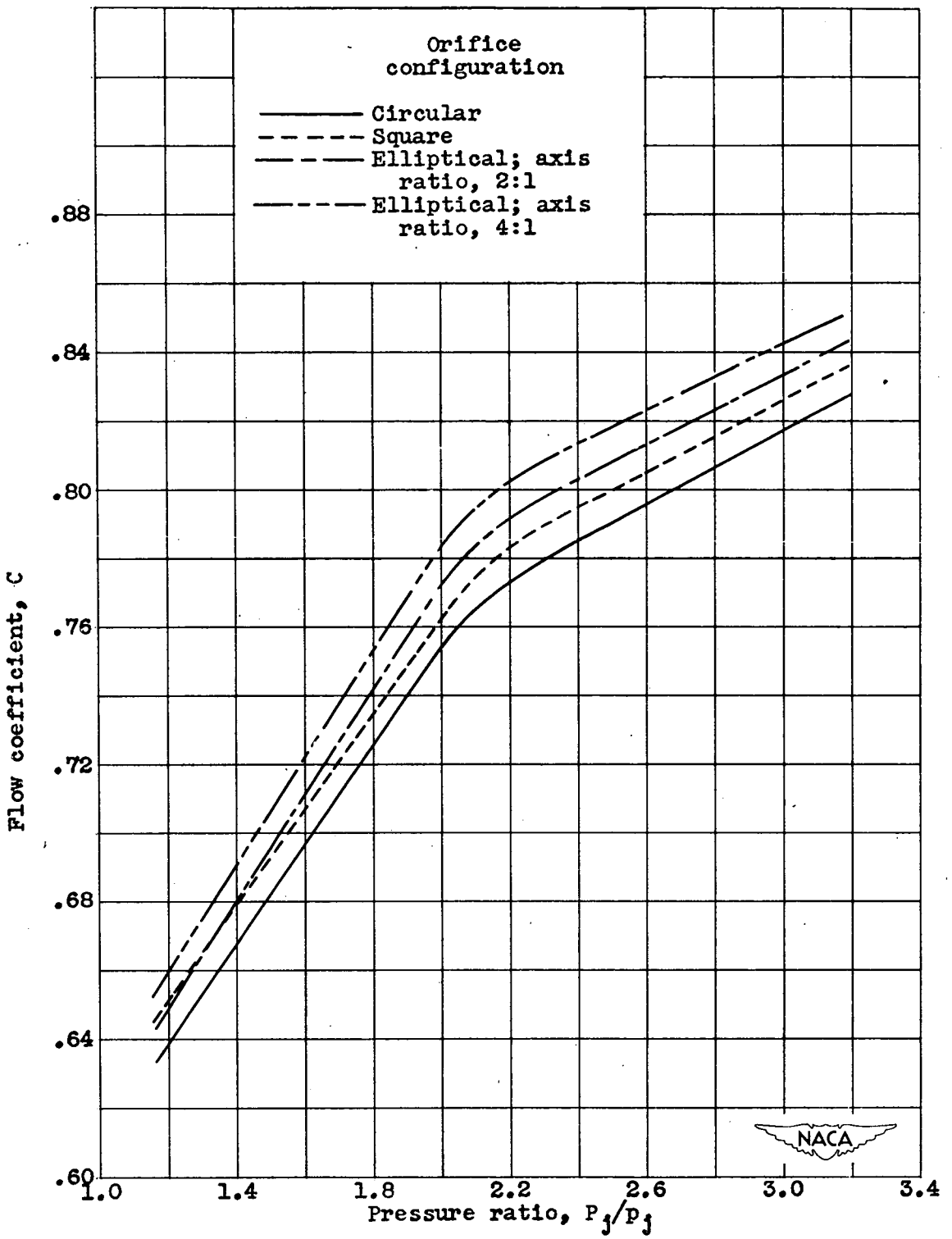

Figure 12. - Comparison of variation of calculated flow coefficient with pressure ratio for circular, square, and elliptical orifices. Orifice area, 0.307 square inch; jet total temperature, 4000° F; outlet pressure, 2116 pounds per square foot.

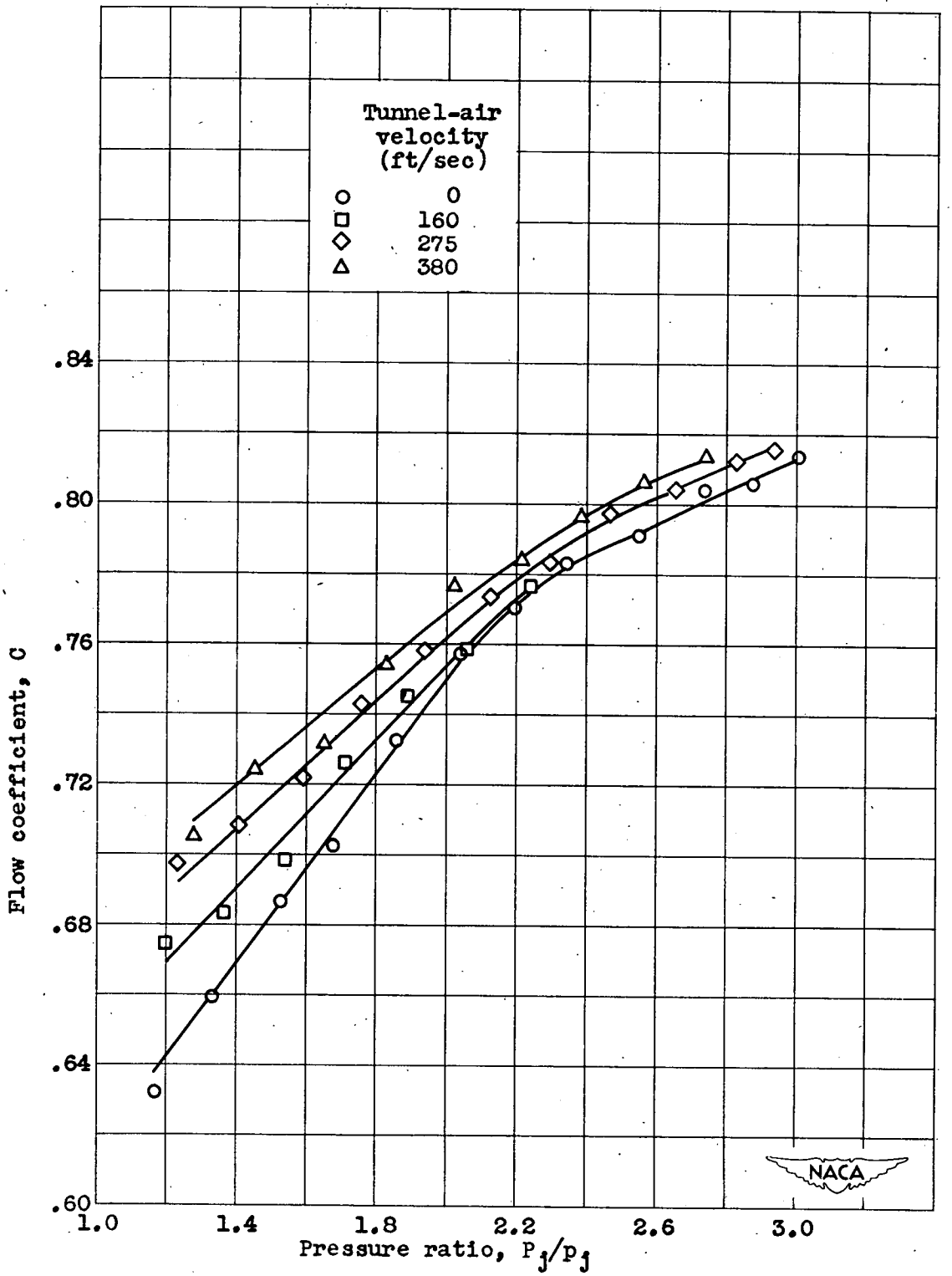

Figure 13. - Variation of uncorrected flow coefficient with uncorrected pressure ratio for 0.625-inch circular orifice at several tunnel-air velocities. Jet total temperature, 400° F.

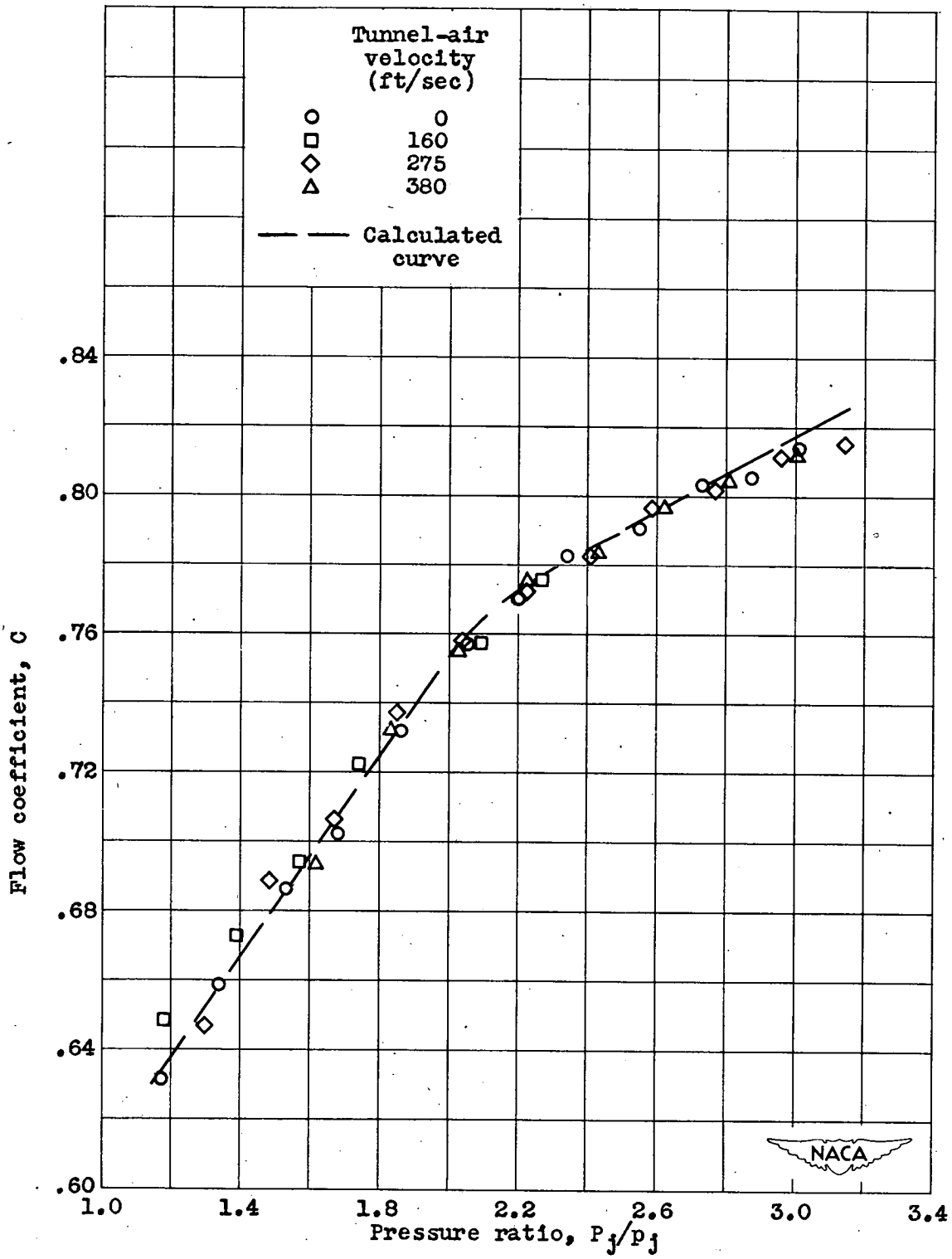

Figure 14. - Variation of corrected flow coefficient with corrected pressure ratio for 0.625-inch circular orifice at several tunnel-air velocities. Jet total temperature, 400° F.